Research letter

Characteristics of an airfoil with stationary vortices

P. Ranjan & R. E. Breidenthal

University of Washington

William E. Boeing Department of Aeronautics and Astronautics

Box 352400 Seattle, WA 98195-2400 USA

breident@aa.washington.edu

Abstract

The aerodynamic performance of a NACA 0016 airfoil with stationary vortices is explored. Vortex generators are positioned near the leading edge on the suction side of the airfoil. The resulting vortices are stabilized by streamwise grooves. For a certain configuration of the vortex generators and the streamwise grooves, the flow remains essentially attached up to an angle of attack of 25 degrees, much greater than the normal 14 degrees for the unmodified airfoil at Re = $9x10^5$. Consistent with attached flow, the drag coefficient measured from the wake momentum is remarkably low at large angles of attack. Stationary vortices provide a new method for inhibiting boundary layer separation.

1. INTRODUCTION

Maintaining attached flow at high angles of attack is desirable for many aerodynamic applications. Flows separate because of positive pressure gradients preferentially decelerating the low-momentum fluid near the wall, according to the nonlinear Euler equation for frictionless flow

$$dp = -\rho u du \tag{1}$$

where p is the pressure, ρ is the density, and u is the streamwise velocity. While frictional effects set the stage by establishing the initial boundary layer velocity profile, the essential physics of separation is described by the nonlinear Euler equation. Where u is small near the wall, the deceleration du is relatively large in magnitude for a given pressure rise dp. If the low-momentum fluid near a wall can either be reduced in extent, or if the transport of momentum into that region can be increased, then boundary layer separation can be inhibited.

Recent discoveries have revealed that stationary vortices have fundamentally different behavior from nonstationary ones. Cotel [1] attributed a strong dependence of the entrainment rate across a stratified surface to the stationarity of a nearby vortex. This assertion was further supported by Cotel [2], who demonstrated a reduction in entrainment rate by up to two orders of magnitude for a precessing jet as compared to that of a vertical jet, consistent with their theory.

For the purposes of this brief note, it is sufficient to describe the basic theoretical idea. There are two important eddy scales in classical turbulent flow, the largest and the smallest. Corresponding to these two scales, there are two important limits in the ratio T of the rotational to translational velocity of a eddy near a surface. In the limit of T >> 1, the vortex is stationary, or “persistent”. In the other limit, T << 1, the vortex is nonstationary. If the surface is such that the velocity goes to zero there, all fluxes across that surface must be diffusive. From dimensional considerations, all fluxes must be proportional to $(\nu/\tau)^{1/2}$, where ν is the diffusivity (in this case of momentum) and τ is the rotation period of some vortex. The theory asserts that if the flow is stationary, then the correct choice for τ is that of the largest eddy, and the flux is essentially laminar. If nonstationary, then τ is that of the smallest eddy, the Kolmogorov microscale, and the flux is turbulent.

In order to test the theory, stationary vortices were placed near a solid surface. However, in order to achieve stationary vortices, the surface cannot be flat, as the image vortices make the system unstable to short-wave Widnall [3] and long-wave Crow [4] instabilities. Balle [5] and Kier [6] proposed a wavy wall to help stabilize the vortices. A corrugated plate with a sinusoidal shape was placed in a water tunnel, with the grooves nearly aligned with the freestream direction. Flow visualization revealed that an initially turbulent boundary layer was relaminarized by the addition of stationary vortices over about half of each wave, Dawson [7], with a flow pattern resembling Kelvin's cats' eyes.

Because of the relaminarization, surface fluxes are expected to be reduced. Indeed, the heat transfer coefficient at the bottom of the trough was observed to be reduced to laminar values (Balle [5]).

2. APPLICATION TO AN AIRFOIL

If stationary vortices on the suction side of a lifting airfoil have reduced skin friction, then the boundary layer will be thinner as it approaches the trailing edge. According to Euler's equation (1), the region of anemic momentum susceptible to large deceleration by the positive pressure gradient will therefore be reduced.

Even if relatively thin, however, laminar boundary layers are nonetheless vulnerable to separation. There is little transport of momentum toward the wall from the high-speed, outer flow.

In order to inhibit separation, it is therefore desirable to exploit the reduced skin friction of stationary vortices over some forward section of the suction side, but to increase the transport of momentum toward the wall approaching the trailing edge. This might be achieved by terminating the wavy wall stabilization just before the boundary layer would otherwise separate. Without the stabilization, the vortices should become unstable and increase the transport rate of high-momentum fluid toward the surface.

In order to help stabilize the streamwise vortices, we add streamwise ridges (or grooves) to the airfoil. The geometry and underlying physics should be distinguished from the case of spanwise grooves, such as corrugated dragonfly airfoils. According to the literature, the spanwise corrugations in low Reynolds number, dragonfly-type airfoils inhibit boundary layer separation by enhancing the turbulent transport of high momentum toward the wall (Tamai [8], Gao [9], Hu [10] and Murphy [11]). In contrast, the streamwise grooves in the present work are designed to inhibit momentum transport.

3. EXPERIMENTAL SETUP

Details of the wavy wall configuration are explained elsewhere (Balle & Breidenthal 2002)[5]. A NACA 0016 airfoil nearly spanned the test section in a 3x3 foot wind tunnel and tested at speeds in the range 40-60 m/s or Re = 6×10^5 - 9×10^5 based on airfoil chord length. The airfoil chord was 0.381 m (15 inches). The wake momentum was measured with a rake consisting of 48 pitot tubes about one chord length downstream from the trailing edge of the airfoil. The position of the rake was selected to capture the complete wake even at high angles of attack.

Sinusoidal grooves were built up on the suction side of the airfoil with clax, a clay-wax mixture commonly used in wind tunnel testing. The grooves were yawed by about one degree throughout the experiments to account for the spanwise movement of the vortices from their self-induced motion. The airfoil is held vertically inside the test section by two circular plates of diameter 0.5 m (20 inches) at each tip of the airfoil. The wavy wall started at 0.076 m (3 inches) from the leading edge, allowing space for the flow to accelerate as well as for installing the vortex generators. The grooves terminated 0.05 m (2 inches) before the leading edge of the airfoil so that the vortices could become unstable before the flow would otherwise separate. Figure 1 illustrates a numerical model of the geometry.

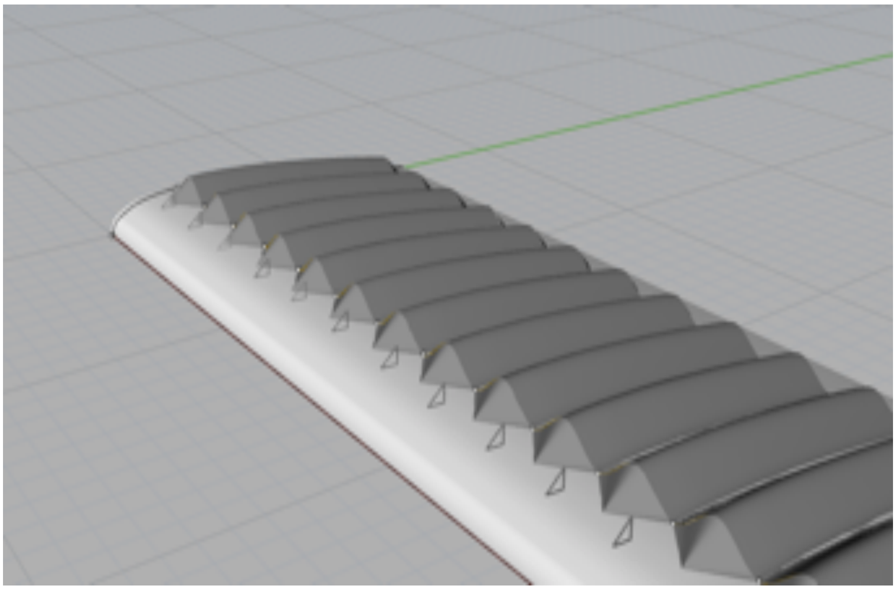

Figure. 1 Computer-aided design model for wavy airfoil.

An array of co-rotating vortices was generated from VG's fabricated from 0.00038 m (0.015") stainless steel sheet. The identical VG's were half-delta wings installed at about the quarter chord station of the airfoil. The angle of attack of the VG's remained fixed during the experiment. Each vortex was approximately centered in its respective trough.

4. RESULTS

Three different wavy walls were constructed, and VG's with heights ranging from 0.013-0.017 m (0.55 - 0.7 inches) were explored. The stalling angle was detected using flow visualization of tufts. After numerous iterations, the configuration with the largest stalling angle was achieved with the parameters listed in table 1.

Table 1: (a) VG specifications (b) Wavy wall specifications

VG specifications

VG height (m)	Base Span (m)	VG chord (m)	VG angle of attack α_{VG} (degs)
0.019	0.022	0.038	+19

Wavy wall specifications

Amplitude (m)	Wavelength (m)	Chordwise length (m)	α_{WW} (degs)

0.017	0.063	0.203	+3

For the optimum geometry, at each airfoil angle of attack, the rake is moved both upward and downward from the airfoil centerline position with an increment of 0.0063 m (0.25") (quarter of the wavelength) to calculate a spanwise C_d distribution. Figure 2 illustrates the c_d distribution at $Re = 6\times10^5$ or $U_\infty = 40$ m/s and $Re = 9\times10^5$ or $U_\infty = 60$ m/s for $\alpha = +12$ degrees. Each value of c_d in the figure corresponds to a station present either at the crest, trough or at a quarter wavelength.

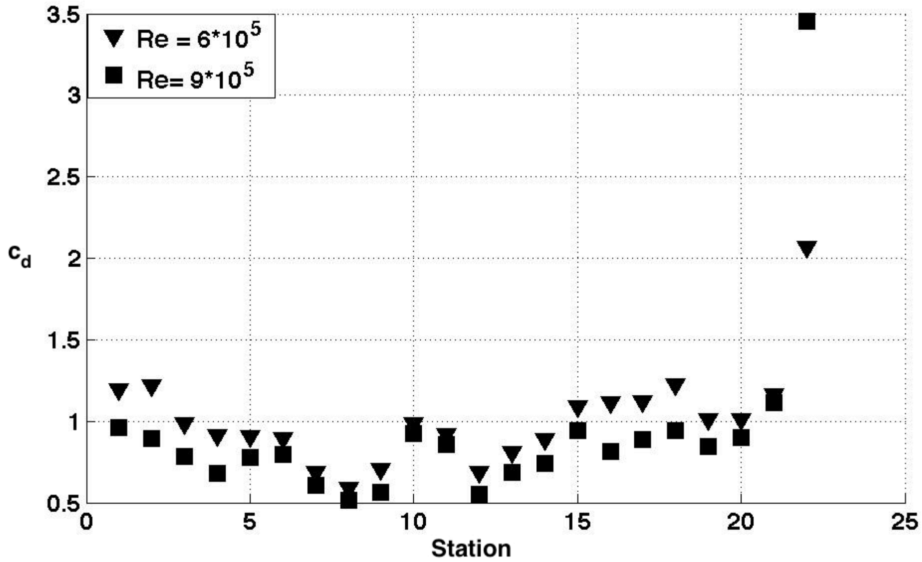

Figure. 2 Spanwise distribution of c_d at α = +12 degrees.

Sullivan [12] studied different wavy airfoil configurations such as a wavy wall at both upper and lower surfaces, a wavy wall at only upper surface, high amplitude and low wavelength geometries, each having a significant effect on airfoil characteristics. Though turbulators and VG's were used initially, their proposed design consisted of only a wavy wall without VG's on the airfoil surface. In the current study, the airfoil with only a wavy wall is also studied. Figure 3 shows the spanwise distribution of c_d for the airfoil wavy wall devoid of VG's at velocities ranging from 40-60 m/s. At large angles of attack, the drag coefficient with the stationary vortices is much less than the unmodified airfoil.

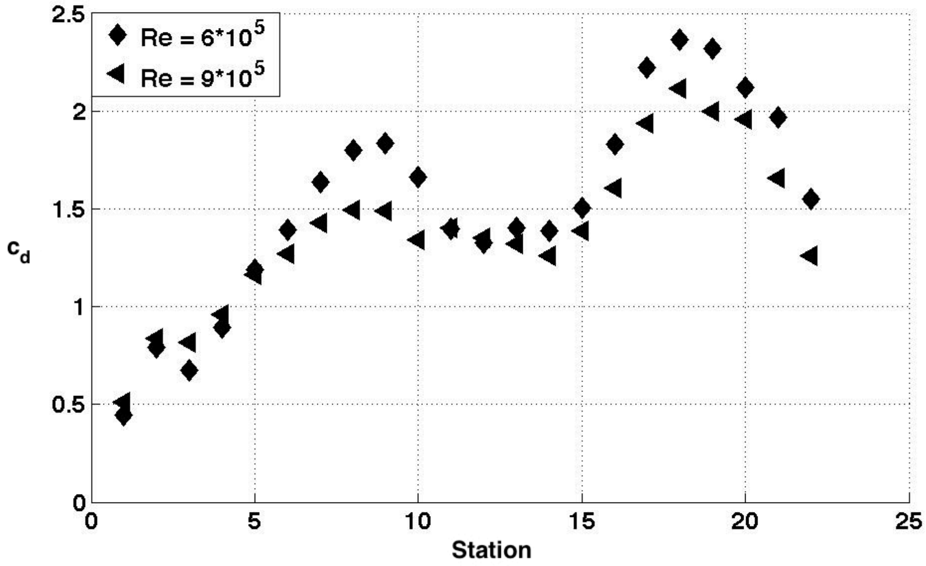

Figure. 3 Spanwise distribution of c_d at $\alpha = +12^0$ for a wavy airfoil without VG's.

Since the wavy surface extended over only the central 60% of the total airfoil span, unsteady flow at large angles of attack was observed near the tips of the airfoil. In Figures 2 and 3, the result of such effects are seen in terms of high values of c_d for stations not in the proximity of airfoil centerline (station 11). The optimum wavy airfoil configuration is compared with a plain NACA 0016 airfoil (Figure 4). Here, the position of the rake is fixed at the airfoil centerline, i.e. at station 11.

The results indicate that the drag coefficient decreases as the Reynolds number increases.

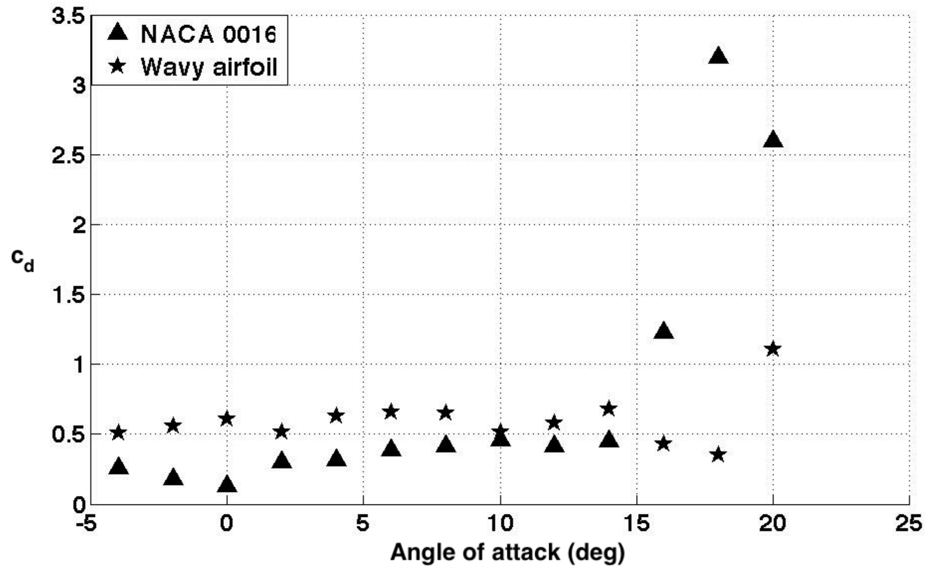

Figure. 4(a) c_d vs. angle of attack for NACA 0016 airfoil and wavy airfoil with VG's at $Re = 6*10^5$.

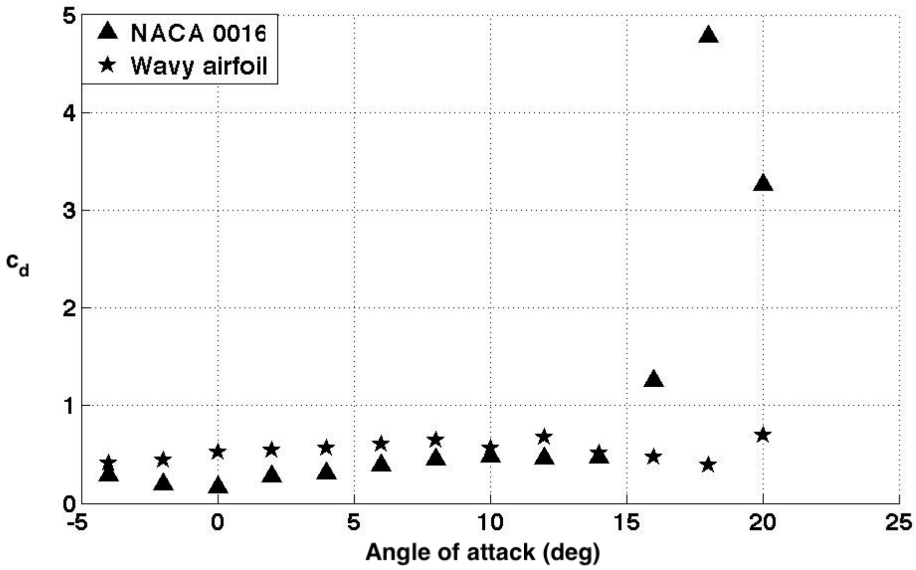

Figure. 4(b) c_d vs. angle of attack for NACA 0016 airfoil and wavy airfoil at Re = $9*10^5$.

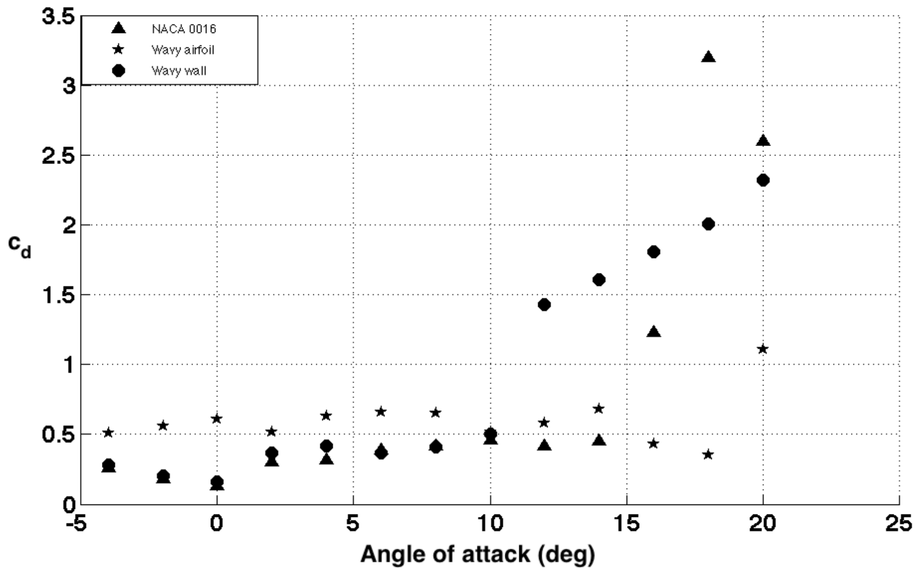

Figure. 5. c_d vs. angle of attack for various configurations at Re = $6*10^5$.

5. CONCLUSION

The addition of stationary vortices on an airfoil can inhibit boundary layer separation, increase the stalling angle of attack, and reduce the drag at high lift coefficients. For the best configuration tested, the flow remained attached until 25 degrees angle of attack, in comparison to the unmodified airfoil's separation at 14 degrees.

The current study only presents data obtained from wake analysis. Due to lack of both time and equipment, the airfoil surface pressure distribution was not calculated. A force balance was also not available. Hence c_l could not be measured. Also, the wake momentum method of drag limited the measurements to about 18 degrees angle of attack or less. However, the observed flow attachment achieved at higher angles of attack would appear to satisfy the Kutta condition. From the theory of lift, the lift coefficient there would be corresponding large. If the drag is relatively low there, large values of the lift-to-drag ratio L/D may find useful application in high-lift applications, especially if wing flap systems can be simplified or even eliminated in an airplane design. Another possibility is that the stationary vortices might only be deployed on the flaps; so that they do not cause drag during cruise flight, where high lift coefficients are not necessary.

Note that for wind and water turbines, the figure of merit is $c_l^{3/2}/c_d$ instead of the more familiar c_l/c_d for airplane applications, since the energy is "free". Thus even if the stationary vortex airfoil does not outperform conventional airfoils in terms of c_l/c_d, it may do so for $c_l^{3/2}/c_d$.

Based on these exploratory measurements, future testing is planned at higher Reynolds number. The effects of freestream turbulence and yaw are also outstanding questions.

ACKNOWLEDGEMENT

The authors are pleased to thank Mr. Robert Gordon for all his help in the wind tunnel.

REFERENCES

[1]	Cotel AJ, Breidenthal RE (1994) Persistence Theory stratified entrainment. Reprints of the fourth International Symposium on stratified flows 4 Grenoble, France, June 29-July 2, 1994.
[2]	Cotel AJ, Gjestvang JA, Ramkhelawan NN, Breidenthal RE (1997) Laboratory experiments of a jet impinging on a stratified interface. Exp Fluids 23:155-160.
[3]	Windall SE, Bliss DB, Tsai C-Y (1974) The instability of short waves on a vortex ring. J. Fluid Mech 66:35-47.
[4]	Crow SC (1970) Stability theory of a pair of trailing vortices. AIAA J 8:2172-2179.
[5]	Balle GJ, Breidenthal RE (2002) Stationary vortices and persistent turbulence in Karman grooves. J. Turbulence 3:33-51.
[6]	Theimo Matthias Kier (1999) Vortex behavior near a corrugated wall. Master's thesis, University of Washington.
[7]	Dawson OR (2005) The effect of persistent vortices on boundary layer behavior in glow along a wavy wall. M.S thesis, University of Washington.
[8]	Tamai M, Wang Z, Rajagopalan G, Hu H (2007) Aerodynamic Performance of a Corrugated Dragonfly Airfoil Compared with Smooth Airfoils at Low Reynolds Numbers. 45th AIAA Aerospace Sciences Meeting and Exhibit, 8-11 January, 2007.
[9]	Gao H, Hu H, Wang Z.J (2008) Computational Study of Unsteady Flows around Dragonfly and Smooth Airfoils at Low Reynolds Numbers. 46th AIAA Aerospace Sciences Meeting and Exhibit, 7-10 January, 2008.
[10]	Hu H, Tamai M (2008) Bioinspired Corrugated Airfoil at Low Reynolds Numbers. J. Aircraft Vol.45, No.6, Nov-December 2008.
[11]	Murphy J, Hu H (2009) An Experimental Investigation on a Bio-inspired Corrugated Airfoil. 47th AIAA Aerospace Sciences Meeting Including the New Horizons Forum and Aerospace Exhibit, 5-8 Jan 2009.
[12]	J Sullivan, CR Sullivan - US Patent App. 12/807,727, 2010.